Supporting Information

Farwick et al. 10.1073/pnas.1323464111

SI Materials and Methods

Strains and Media. Strains and plasmids used in this work are listed in Tables S2 and S3.

Saccharomyces cerevisiae was grown in yeast extract peptone (YEP) medium (10 g/L yeast extract, 20 g/L bacteriological peptone), synthetic complete (SC) medium (1.7 g/L yeast nitrogen base without amino acids and ammonium sulfate, 5 g/L ammonium sulfate, amino acid supplements), or synthetic minimal (SM) medium (same as SC, but without amino acid supplements and with 20 mM monopotassium phosphate) at 30 °C. Synthetic media were adjusted to pH 6.3 with potassium hydroxide and were supplemented with uracil, L-leucine, L-tryptophan, and L-histidine as needed for selection of auxotrophic plasmid markers (1). G418 (200 μg/mL), hygromycin B (200 μg/mL), and clonNAT/nourseothricin (100 μg/mL) were added for selection of *kanMX*, *hphNT1*, and *natNT2* markers, respectively. If not stated otherwise, carbon sources were added to concentrations of 20 g/L [glucose (D), ethanol (E), galactose (G)] or 10 g/L [xylose (X), maltose (M)]. EBY.VW4000 was cultured on maltose or ethanol, AFY10 and AFY10X on ethanol.

Plasmids were amplified in *Escherichia coli* strains DH5α (Gibco BRL) and SURE (Stratagene). *E. coli* was grown in lysogeny broth (LB) at 37 °C or 30 °C (for *HXT7* plasmids) with 100 μg/mL ampicillin or 50 μg/mL kanamycin for plasmid selection.

Transformation and DNA Preparation. *E. coli* transformations were performed via electroporation according to the method of Dower et al. (2). Plasmids were isolated from *E. coli* using the GeneJET Plasmid Miniprep Kit (Fisher Scientific). *S. cerevisiae* was transformed according to protocols by Gietz et al. (3, 4). DNA from *S. cerevisiae* for plasmid recovery, PCR analysis of mutant transporter ORFs, or verification of genomic gene deletions/integrations was isolated as described in ref. 5.

Plasmid Construction. Plasmids were constructed in vivo by homologous recombination in *S. cerevisiae* as described in ref. 6. Suitable DNA fragments were generated by PCR using primers with a 5′ sequence homologous to the integration region in the vector backbone (Table S4). Plasmids were linearized by restriction digestion. Assembled plasmids were recovered from yeast DNA preparations by *E. coli* transformation, clone selection, and plasmid isolation. Constructs were verified by restriction digestion analysis and DNA sequencing of the ORF. *HXT7* and *GAL2* were amplified from CEN.PK2-1c genomic DNA (sequences identical to CEN.PK113-7D).

For easy separation of transporter-coding plasmids and the xylose isomerase (XI)-coding plasmid, the ORF of the ampicillin resistance in YEp181_pHXT7-optXI_Clos (7) was replaced by the kanamycin resistance gene from pDONR222 (Invitrogen).

The integrative plasmid pAF-HD8.3 was generated from pHD8 (8) by successive excision of *HXT7* and opt*xylA*, and the 2μ origin by restriction digestion, religation of the vector, amplification in *E. coli*, and confirmation by restriction digestion analysis.

Strain Construction. Genes were targeted by the homologous regions flanking the deletion cassettes. For *HXK1* and *YLR446W*, *hphNT1* cassettes were amplified from plasmid pZC1 using primers containing the homologous sequence in their 5′ part. *KanMX* cassettes for deletion of *GLK1* and *HXK2* were amplified from genomic DNA of preexisting deletion strains (7), resulting in cassettes with extended homologous regions (200–300 bp), which increases target efficiency. All genome integrations and deletions were confirmed by PCR analysis. For cassette removal, we relied on the low basal expression of cre recombinase from plasmid pSH47 on maltose or ethanol medium because full induction by galactose is lethal to EBY.VW4000 due to multiple *loxP* sites across the genome. Removal of cassettes was confirmed by PCR. The *hxk*^{0}-phenotype in the *hxt*^{0} background was verified on maltose media. Maltose is transported by specific transporters that are still present in the *hxt*^{0} strain (Mal21, Mal31) and is then cleaved into two glucose monomers. Disruption of the hexo- and glucokinase genes prevents maltose utilization. Codon optimization is described in ref. 9. Primers are listed in Table S4.

epPCR Mutagenesis. The GeneMorph II Random Mutagenesis Kit (Agilent Technologies) was used for error-prone PCR (epPCR) mutagenesis of *GAL2* and *HXT7* with low (0–4.5 mutations per kb), medium (4.5–9 mutations per kb), and high (9–16 mutations per kb) mutation frequencies. epPCR was performed with primer pairs Amp_GAL2_F/R and Amp_HXT7_F/R, with p426_GAL2 and p426_HXT7 as templates, respectively. The epPCR fragments were purified by agarose-gel electrophoresis and gel extraction (NucleoSpin Extract II; Macherey-Nagel) and used as templates for a PCR with primer pairs Clon_GAL2_F/R and Clon_HXT7_F/R to prepare fragments for recombinational cloning. AFY10X was transformed with linearized p426H7 and the PCR products and then screened as described in *Clone Selection and Analysis* in the *Materials and Methods* section of the main text.

Site-Directed Mutagenesis. Mutations were inserted into *HXT7* or *GAL2* by site-directed PCR mutagenesis in combination with in vivo recombinational cloning. Two fragments of the ORF, overlapping at the target site, were amplified from the wild-type-plasmids. Two mutagenesis primers covered the target codon and the neighboring 15–20 nucleotides and were directed in opposing directions (forward and reverse). They were combined with the respective reverse and forward cloning primers (as used for the wild type) in separate PCRs. Mutant constructs were assembled from the two fragments and a pRS62N vector backbone by homologous recombination directly in the screening strain AFY10X. The screening procedure is described in *Clone Selection and Analysis* in the *Materials and Methods* section of the main text. Single amino acid mutations were done accordingly, but in EBY.VW4000.

Primers for (semi)random mutagenesis were used as equal mixtures of oligonucleotides with variations at one or more positions of the target codon (expressed in ambiguity code in the primer sequence). The threonine 219/213 codon in both ORFs was altered in three separate sets (defined by three sets of mutagenesis primers), grouping amino acid changes from threonine to alanine/glycine/valine (codon gbt), serine/cysteine (codon tst), and asparagine/aspartic (codon rac). The asparagine 376/370 residue was randomly changed to the 20 proteinogenic amino acids (codon nnn). All primers are listed in Table S4.

Uptake Assays. EBY.VW4000 containing the respective plasmid was grown in selective yeast extract peptone ethanol (YEPE) to an OD_{600} of 1.1–1.6, harvested by centrifugation, and washed twice in ice-cold uptake buffer (100 mM potassium phosphate, pH 6.5). Cell suspensions of 60 $mg_{wetweight}$/mL were prepared in uptake buffer, aliquotted, and stored on ice. For each measurement, 50 μL of 3× concentrated sugar solution and 100 μL of cell suspension were equilibrated to 30 °C for 4–5 min and then mixed. After 5 s (glucose) or 20 s (xylose), 100 μL of the mixture

were pipetted into 10 mL of ice-cold quenching buffer (100 mM potassium phosphate, 500 mM glucose, pH 6.5) to stop the reaction. Cells were filtered through a Durapore membrane filter with a 0.22-μm pore size (Millipore) and washed twice with 10 mL of ice-cold quenching buffer. The filter was transferred to a scintillation vial containing 4 mL of Rotiszint eco plus (Roth). Then, 10 μL of each reaction were transferred directly to a scintillation vial with 4 mL of scintillation mixture for determination of the total counts in each reaction. To determine a value for sugar that is unspecifically bound to the cell surface or the filter, samples of 33.3 μL of sugar solution and 66.6 μL of cell suspension were mixed in 10 mL of ice-cold quenching buffer and then treated as described for the other samples. Radioactivity was analyzed in a Wallac 1409 liquid scintillation counter.

Uptake was measured at sugar concentrations 0.2, 1, 5, 25, and 100 mM for glucose and 1, 5, 25, 66, 100, 200, and 500 mM for xylose. Inhibition of xylose uptake by glucose was measured at 25, 66, and 100 mM xylose with additional 25 and 100 mM unlabeled glucose. Sugar solutions contained 0.135–0.608 μCi of D-[U-^{14}C]-glucose (290-300 mCi/mmol) or D-[1-^{14}C]-xylose (55 mCi/mmol) (American Radiolabeled Chemicals). Calculation of K_m (Michaelis constant), V_{max} (maximal initial uptake velocity), and K_i (inhibitor constant for competitive inhibition) was done by nonlinear regression analysis and global curve fitting in Prism 5 (GraphPad Software) with values of three independent measurements.

1. Zimmermann FK (1975) Procedures used in the induction of mitotic recombination and mutation in the yeast *Saccharomyces cerevisiae*. *Mutat Res* 31(2):71–86.
2. Dower WJ, Miller JF, Ragsdale CW (1988) High efficiency transformation of *E. coli* by high voltage electroporation. *Nucleic Acids Res* 16(13):6127–6145.
3. Gietz RD, Schiestl RH (2007) Frozen competent yeast cells that can be transformed with high efficiency using the LiAc/SS carrier DNA/PEG method. *Nat Protoc* 2(1):1–4.
4. Gietz RD, Schiestl RH (2007) High-efficiency yeast transformation using the LiAc/SS carrier DNA/PEG method. *Nat Protoc* 2(1):31–34.
5. Sambrook J, Russell DW (2001) *Molecular Cloning: A Laboratory Manual* (Cold Spring Harbor Lab Press, Plainview, NY), 3rd Ed.
6. Oldenburg KR, Vo KT, Michaelis S, Paddon C (1997) Recombination-mediated PCR-directed plasmid construction in vivo in yeast. *Nucleic Acids Res* 25(2):451–452.
7. Subtil T, Boles E (2012) Competition between pentoses and glucose during uptake and catabolism in recombinant *Saccharomyces cerevisiae*. *Biotechnol Biofuels* 5(1):14.
8. Demeke MM, et al. (2013) Development of a D-xylose fermenting and inhibitor tolerant industrial *Saccharomyces cerevisiae* strain with high performance in lignocellulose hydrolysates using metabolic and evolutionary engineering. *Biotechnol Biofuels* 6(1):89.
9. Wiedemann B, Boles E (2008) Codon-optimized bacterial genes improve L-Arabinose fermentation in recombinant *Saccharomyces cerevisiae*. *Appl Environ Microbiol* 74(7): 2043–2050.

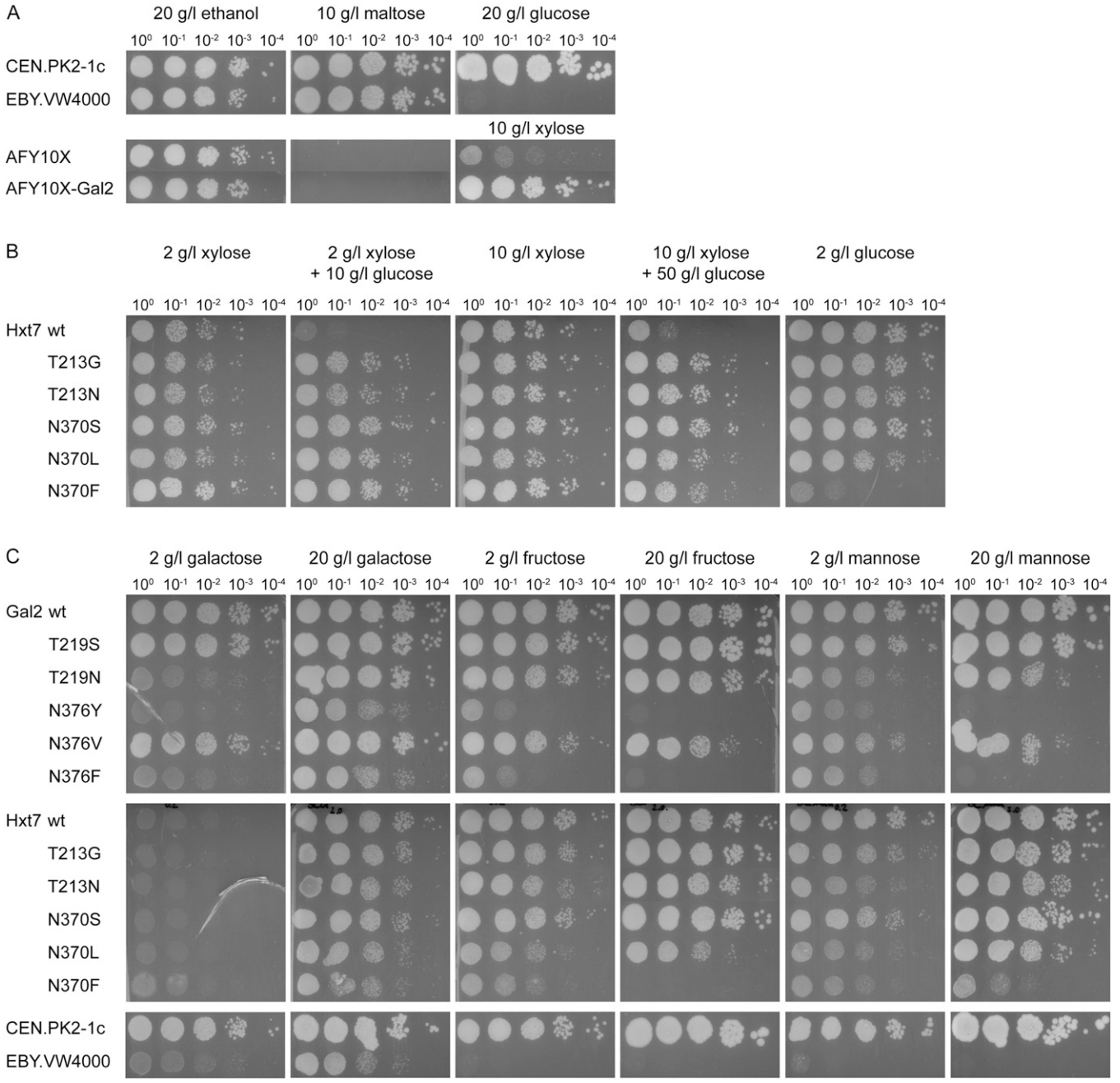

Fig. S1. (*A*) Growth analysis of the screening strain AFY10X and its ancestors. All strains were pregrown in liquid selective synthetic complete ethanol (SCE) medium. Serial dilutions of washed cells were dropped on solid SC media with the indicated carbon sources. Cells were grown at 30 °C for 3 d (glucose, maltose) or 6 d (ethanol, xylose). AFY10 was transformed with empty plasmid pRS62N. EBY.VW4000 and CEN.PK2-1c did not grow on xylose, AFY10 and AFY10X did not grow on glucose. (*B*) Functional characterization of Hxt7 wild type and mutants. Growth assay of AFY10X (xylose and xylose–glucose mixtures) and EBY. VW4000 (glucose) overexpressing the indicated transporters. Cells were pregrown in liquid selective SCE or YEPE medium, respectively. Serial dilutions of washed cells were dropped on solid SC media with the indicated carbon sources. Cells were grown at 30 °C for 3 d (glucose) or 6 d (xylose and mixtures). (*C*) Functional characterization of Gal2 and Hxt7 wild type and mutants regarding hexose transport. Growth assay of EBY.VW4000 overexpressing the indicated transporters. Cells were pregrown in liquid selective YEPE medium. Serial dilutions of washed cells were dropped on solid SC media with the indicated carbon sources. Cells were grown at 30 °C for 3 d. CEN.PK2-1c and EBY.VW4000 contain empty plasmid pRS62N.

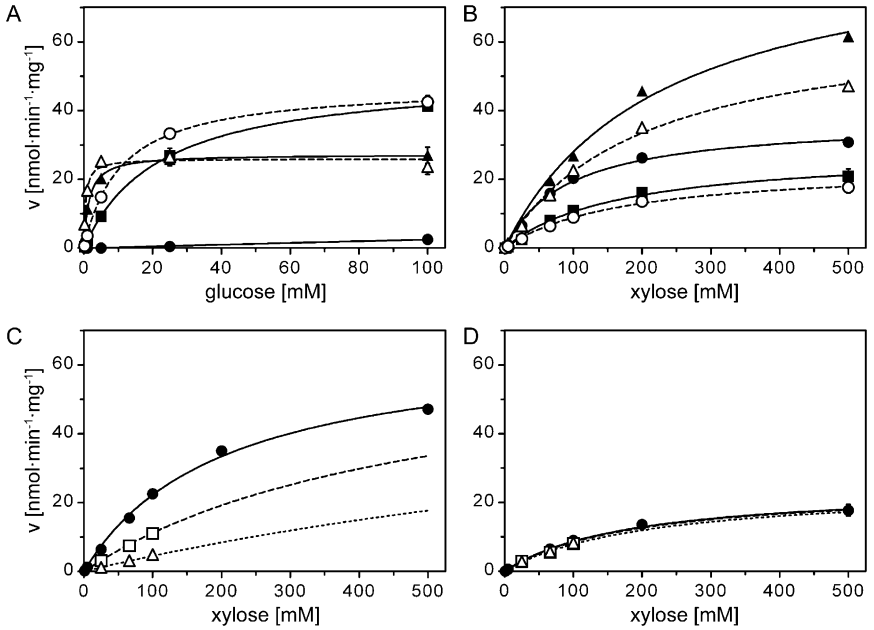

Fig. S2. (*A* and *B*) Glucose (*A*) and xylose (*B*) transport of wild-type and mutant transporters measured in zero-trans influx experiments. EBY.VW4000 overexpressing *GAL2* (solid lines and filled symbols) or *HXT7* (dashed lines and open symbols) variants were grown in selective YEPE. Shown are Gal2 wild type (filled triangle), Gal2-N376F (filled circle), Gal2-N376V (filled square), Hxt7 wild type (open triangle), and Hxt7-N376S (open circle). Curve fitting for Michaelis–Menten kinetics was applied to data of three independent measurements at each concentration. Error bars are given as SEM. Notice the different scales for glucose and xylose concentration. (*C* and *D*) Inhibitory effect of glucose on xylose transport of wild-type and mutant Hxt7. Zero-trans influx of xylose was measured in the absence of glucose (solid line, filled circle) and in the presence of 25 mM (dashed line, open square) or 100 mM glucose (dotted line, open triangle). EBY.VW4000 overexpressing Hxt7 wild type (*C*) or Hxt7-N370S (*D*) was grown in selective YEPE. Global curve fitting for Michaelis–Menten kinetics with competitive inhibition was applied to data of three independent measurements at each concentration. Error bars are given as SEM but are often smaller than the respective symbol. v, initial rate of uptake.

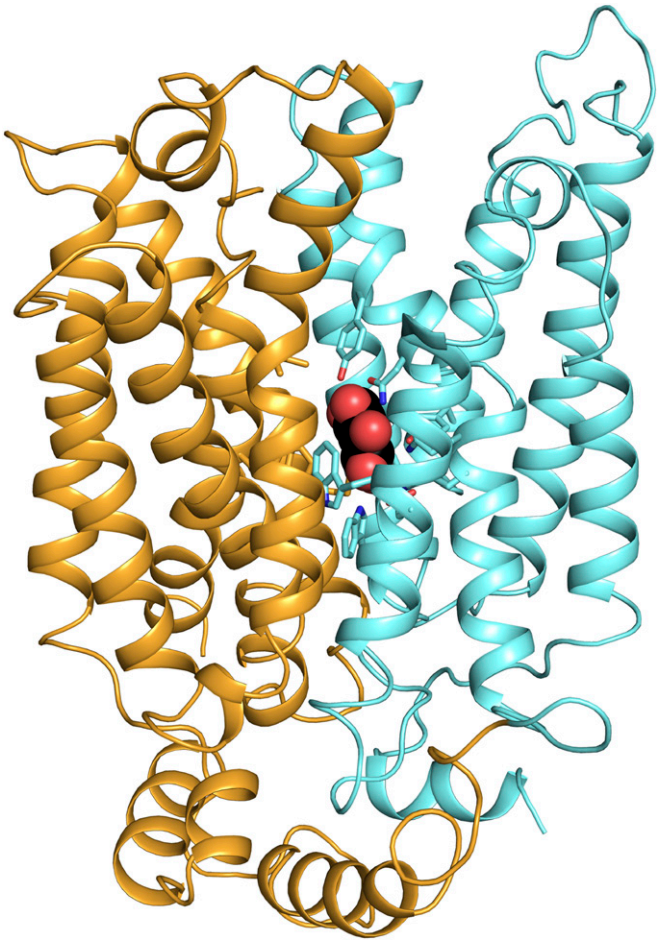

Fig. S3. Homology model of the Gal2 structure generated using the SWISS-MODEL software (1). The model is based on the outward-facing partly occluded structure of *E. coli* XylE with bound glucose (PDB ID code 4GBZ). The N-terminal (amino acids 1–70) and C-terminal (amino acids 536–574) cytosolic tails could not be modeled due to the absence of corresponding sequences in XylE. The side view, with the extracellular side at the top, shows the subdomains N (orange) and C (cyan) and all residues contributing to glucose binding in stick representation. Glucose is shown in space filling model (black and red), and the C6 is oriented to the back. The 3D images were created with PyMOL (2).

1. Arnold K, Bordoli L, Kopp J, Schwede T (2006) The SWISS-MODEL workspace: A web-based environment for protein structure homology modelling. *Bioinformatics* 22(2):195–201.
2. Schrödinger (2010) The PyMOL Molecular Graphics System (Schrödinger, Cambridge, MA), Version 1.3r1.

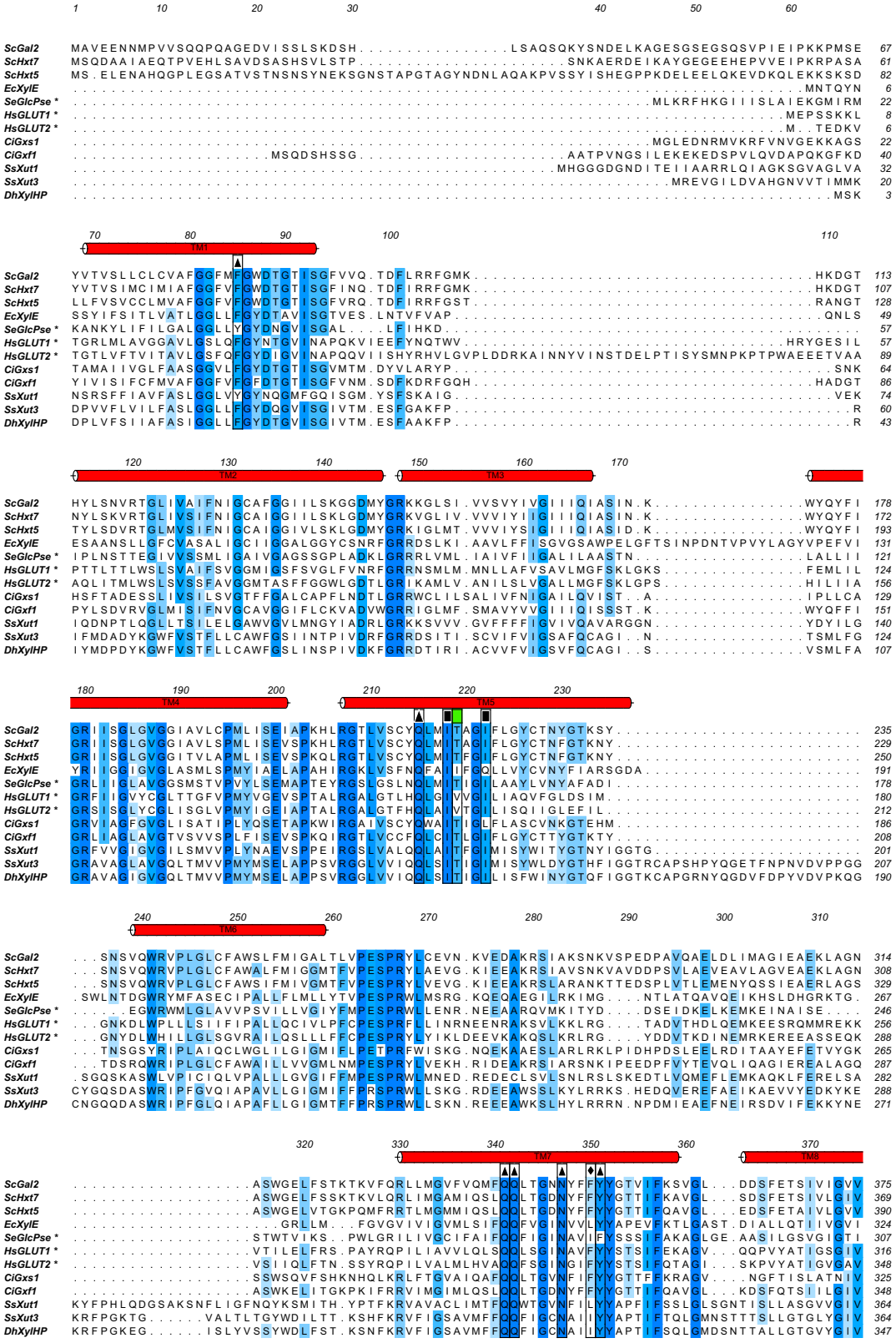

Fig. S4. (Continued)

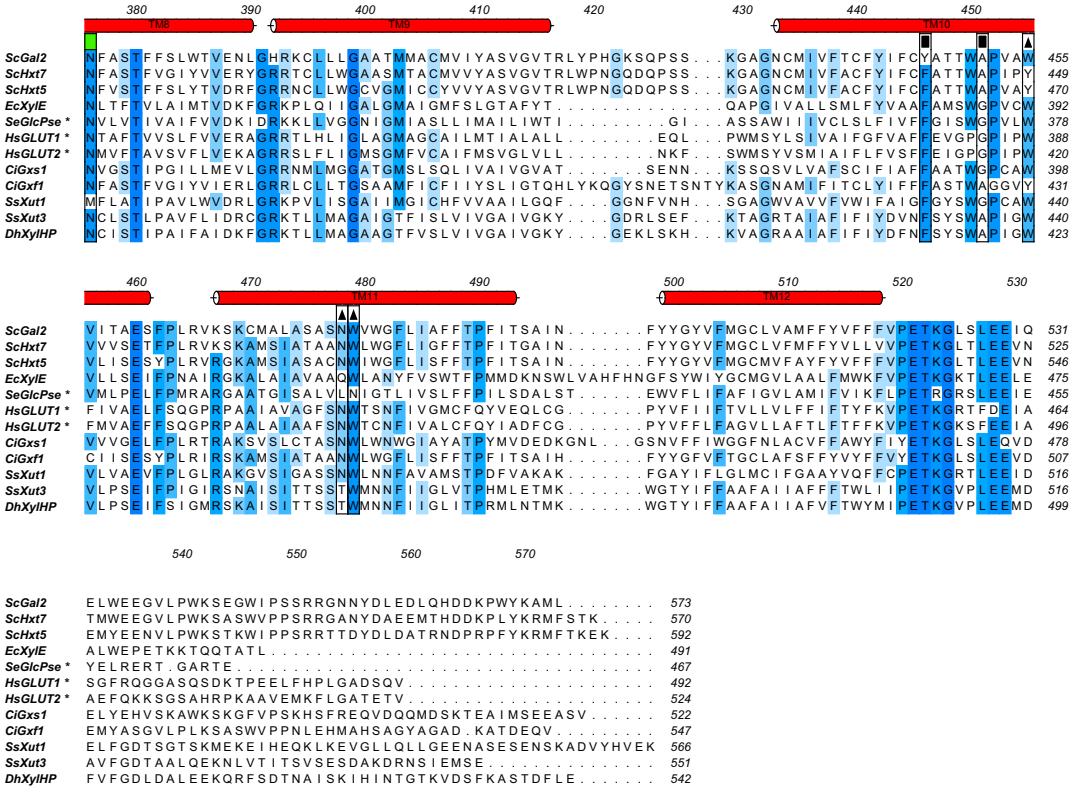

Fig. S4. Protein sequence alignment of different sugar transporters. Transporters mentioned in the main text and additionally further xylose transporters found to be functional in *S. cerevisiae* (1) were aligned using the PRALINE multiple sequence alignment server (2). Transporters aligned are *Saccharomyces cerevisiae* Gal2, Hxt7, and Hxt5, *Escherichia coli* XylE, *Staphylococcus epidermidis* $GlcP_{SE}$, *Homo sapiens* GLUT1 and GLUT2, *Candida intermedia* Gxs1 and Gxf1, *Scheffersomyces stipitis* Xut1 and Xut3, and *Debaryomyces hansenii* xylHP. Transporters not able to transport xylose are marked by asterisks. Transmembrane helices refer to XylE (as adapted from the supporting information of ref. 3). The numbering above refers to the Gal2 sequence. Important residues are boxed, and black symbols indicate their contribution to binding of xylose and glucose (triangle) or glucose only (square), referring to Sun et al. (3). Contribution of F350 (diamond) to glucose binding was inferred from the Gal2 homology model. Green squares indicate the two identified amino acid positions T219/213 and N370/376 in Gal2 and Hxt7, respectively. Similarities of residues are indicated in blue. The figure was created with ALINE software (4).

1. Young E, Poucher A, Comer A, Bailey A, Alper H (2011) Functional survey for heterologous sugar transport proteins, using *Saccharomyces cerevisiae* as a host. *Appl Environ Microbiol* 77(10):3311–3319.
2. Simossis VA, Heringa J (2005) PRALINE: a multiple sequence alignment toolbox that integrates homology-extended and secondary structure information. *Nucleic Acids Res* 33(Web Server issue, suppl 2)W289-94.
3. Sun L, et al. (2012) Crystal structure of a bacterial homologue of glucose transporters GLUT1-4. *Nature* 490(7420):361–366.
4. Bond CS, Schüttelkopf AW (2009) ALINE: a WYSIWYG protein-sequence alignment editor for publication-quality alignments. *Acta Crystallogr D Biol Crystallogr* 65(Pt 5):510–512.

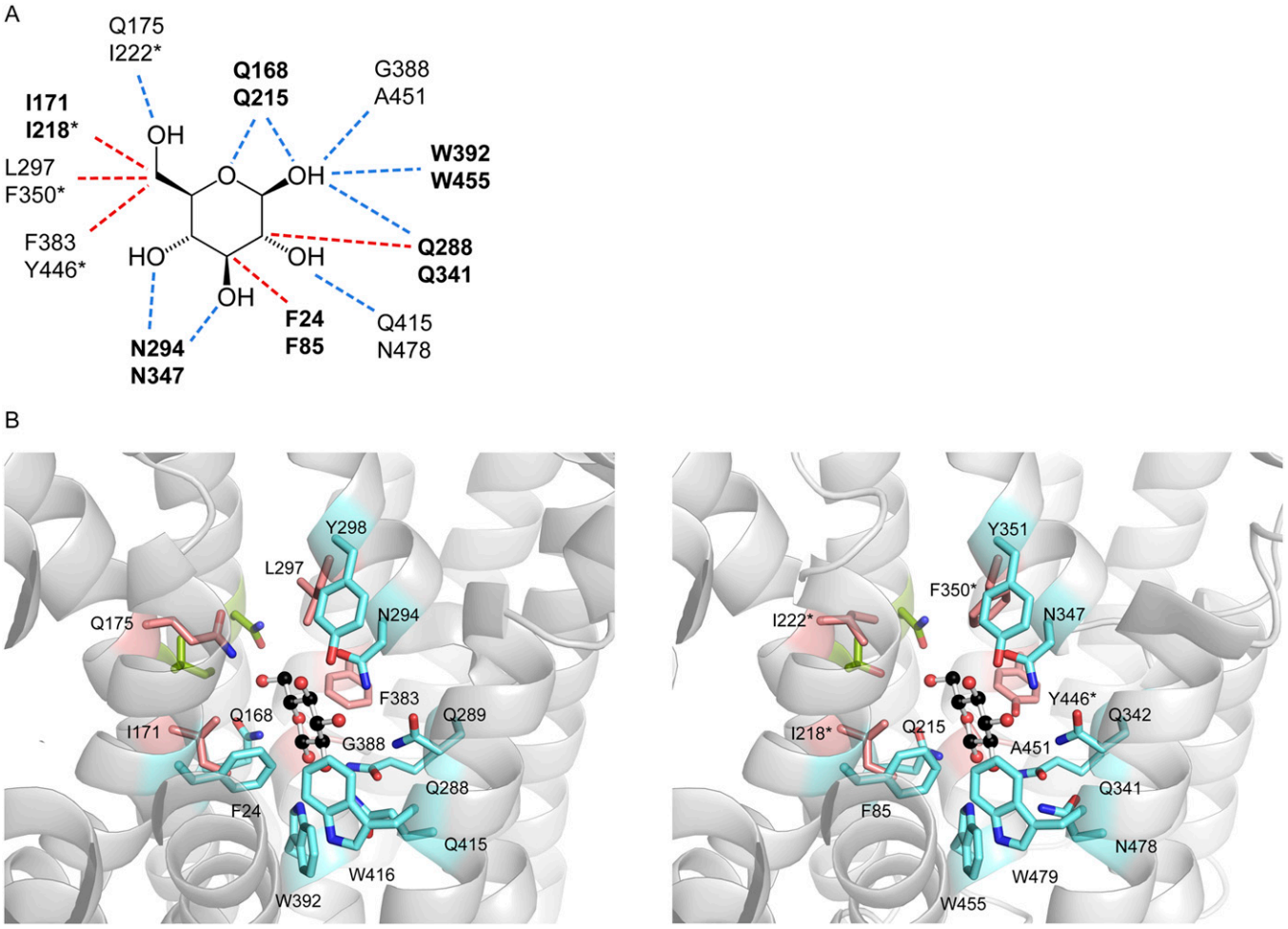

Fig. S5. Sugar coordination of XylE and Gal2. (*A*) Schematic map of glucose coordination in XylE. The residues of the XylE crystal structure (PDB ID code 4GBZ) forming hydrogen bonds (blue) or hydrophobic contacts (red) with β-D-glucose are shown, and the corresponding amino acids of Gal2 are indicated below. The water molecules are omitted for clarity. Conserved residues are indicated in bold. The Gal2 positions that were subjected to site-directed mutagenesis are marked by asterisks. (*B*) A 3D model of the coordination of glucose in the XylE crystal structure (*Left*) and the Gal2 homology model (*Right*). Only TM2, which does not contribute to sugar binding, is omitted for better view of the binding pocket. Residues participating in xylose and glucose binding are indicated in cyan, and residues that exclusively bind to glucose are indicated in salmon. The two identified amino acid positions T219 and N376 in Gal2 and their homologs in XylE (I172 and N325, respectively) are shown in green. The Gal2 positions that were subjected to site-directed mutagenesis are marked by asterisks.

Table S1. Growth of EBY.VW4000 (glucose) and AFY10X (xylose and xylose–glucose mixtures) overexpressing individual Gal2 mutants

Position in			Growth on		
XylE	Gal2	Changed to	Glucose	Xylose	Glucose + xylose
I171	I218	G	—	+	—
		A	+++	+++	—
		D	++	++	—
		F/K	—	—	—
Q175	I222	G/A/D/F/K	—	—	—
		Q	++	++	—
L297	F350	G	+	—	—
		A/Y	++	—	—
		D/K/W	—	—	—
		L	+++	++	—
		M	+++	—	—
F383	Y446	W	—	—	—

Growth was compared with the Gal2 wild type. Growth comparable with the wild type is denoted as (+++), weaker growth with (++) or (+), and no growth as (—).

Table S2. *S. cerevisiae* strains used in this work

Name	Relevant genotype	Source
CEN.PK2-1C	*MATa leu2-3,112 ura3-52 trp1-289 his3Δ1 MAL2-8^{c} SUC2*	E.B. laboratory stocks
EBY.VW4000	CEN.PK2-1C Δ*hxt1-17 gal2Δ::loxP stl1Δ::loxP agt1Δ::loxP mph2Δ::loxP mph3Δ::loxP*	(1)
AFY10	EBY.VW4000 *glk1Δ::loxP hxk1Δ::loxP hxk2Δ::loxP ylr446wΔ::loxP pyk2Δ::pPGK1-opt.XKS1-tPGK1 pTPI1-TAL1-tTAL1 pTDH3-TKL1-tTKL1 pPFK1-RPE1-tRPE1 pFBA-RKI1-tRKI1 loxP*	This work
AFY10X	AFY10, *pHXT7-opt.xylA-tHXT7*, *LEU2* (plasmid YEp-kanR_optXI)	This work

1. Wieczorke R, et al. (1999) Concurrent knock-out of at least 20 transporter genes is required to block uptake of hexoses in *Saccharomyces cervisiae*. *FEBS Lett* 464(3):123–128.

Table S3. Plasmids used in this work

Name	Description	Source
YEp181_pHXT7-optXI_Clos	2μ-plasmid, *LEU2* marker, codon-optimized xylose isomerase gene *xylA* of *C. phytofermentans* (opt.*XylA*) under control of shortened *HXT7*-promoter and *CYC1*-terminator, *E. coli* ampicillin marker	(1)
YEp181-kanR_optXI	2μ-plasmid, *LEU2* marker, codon-optimized xylose isomerase gene *xylA* of *C. phytofermentans* (opt.*XylA*) under control of shortened *HXT7*-promoter and *CYC1*-terminator, *E. coli* kanamycin marker	This work
pDONR222	Gateway-system donor-vector, *E. coli* kanamycin-marker, chloramphenicol-marker, pUC-origin	Life Technologies
pHD8	integrative 2μ-plasmid (*PYK2*-locus), *kanMX* marker, *pHXT7*-opt.*XylA-tCYC1 pPGK1*-opt.*XKS1-tPGK1, pTPI1-TAL1-tTAL1 pTDH3-TKL1-tTKL1, pPFK1-RPE1-tRPE1 pFBA1-RKI1-tRKI1 pPGM1-HXT7-tHXT7*	(2)
pAF-HD8.3	integrative plasmid (*PYK2*-locus), *kanMX* marker, *pPGK1*-opt.*XKS1-tPGK1, pTPI1-TAL1-tTAL1 pTDH3-TKL1-tTKL1 pPFK1-RPE1-tRPE1 pFBA1-RKI1-tRKI1*	This work
pZC1	DNA template for amplification of the *hphNT1*-deletion cassettes	(3)
pSH47	CEN6/ARSH4-plasmid, *URA3* marker, cre-recombinase under control of inducible *GAL1*-promoter and *CYC1*-terminators	(4)
pHL125^{re}	2μ-plasmid; *URA3* marker, *GAL2* under control of *ADH1*-promoter;	(5)
P426H7	2μ-plasmid; *URA3* marker, shortened *HXT7*-promoter and *CYC1*-terminator	(6)
p426_GAL2	ORF of *GAL2* in p426H7	This work
p426_HXT7	ORF of *HXT7* in p426H7	This work
pRS62N	2μ-plasmid; *natNT2* marker; shortened *HXT7*-promoter and *CYC1*-terminator	E.B. laboratory stock
pRS62N_GAL2	ORF of *GAL2* in pRS62N	This work
pRS62N_GAL2-T219S	ORF of *GAL2*-T219S in pRS62N	This work
pRS62N_GAL2-T219N	ORF of *GAL2*-T219N in pRS62N	This work
pRS62N_GAL2-N376Y	ORF of *GAL2*-N376Y in pRS62N	This work
pRS62N_GAL2-N376V	ORF of *GAL2*-N376V in pRS62N	This work
pRS62N_GAL2-N376F	ORF of *GAL2*-N376F in pRS62N	This work
pRS62N_HXT7	ORF of *HXT7* in pRS62N	This work
pRS62N_HXT7-T213G	ORF of *HXT7*-T213G in pRS62N	This work
pRS62N_HXT7-T213N	ORF of *HXT7*-T213N in pRS62N	This work
pRS62N_HXT7-N370S	ORF of *HXT7*-N370S in pRS62N	This work
pRS62N_HXT7-N370L	ORF of *HXT7*-N370L in pRS62N	This work
pRS62N_HXT7-N370F	ORF of *HXT7*-N370F in pRS62N	This work
p426_GAL2-I218G	ORF of *GAL2*-I218G in p426H7	This work
p426_GAL2-I218A	ORF of *GAL2*-I218A in p426H7	This work
p426_GAL2-I218D	ORF of *GAL2*-I218D in p426H7	This work
p426_GAL2-I218K	ORF of *GAL2*-I218K in p426H7	This work
p426_GAL2-I218F	ORF of *GAL2*-I218F in p426H7	This work
p426_GAL2-I222G	ORF of *GAL2*-I222G in p426H7	This work
p426_GAL2-I222A	ORF of *GAL2*-I222A in p426H7	This work
p426_GAL2-I222D	ORF of *GAL2*-I222D in p426H7	This work
p426_GAL2-I222K	ORF of *GAL2*-I222K in p426H7	This work
p426_GAL2-I222F	ORF of *GAL2*-I222F in p426H7	This work
p426_GAL2-I222Q	ORF of *GAL2*-I222Q in p426H7	This work
p426_GAL2-Y446W	ORF of *GAL2*-Y446W in p426H7	This work
p426_GAL2-F350A	ORF of *GAL2*-F350A in p426H7	This work
p426_GAL2-F350D	ORF of *GAL2*-F350D in p426H7	This work
p426_GAL2-F350G	ORF of *GAL2*-F350G in p426H7	This work
p426_GAL2-F350K	ORF of *GAL2*-F350K in p426H7	This work
p426_GAL2-F350L	ORF of *GAL2*-F350L in p426H7	This work
p426_GAL2-F350M	ORF of *GAL2*-F350M in p426H7	This work
p426_GAL2-F350W	ORF of *GAL2*-F350W in p426H7	This work
p426_GAL2-F350Y	ORF of *GAL2*-F350Y in p426H7	This work

1. Subtil T, Boles E (2012) Competition between pentoses and glucose during uptake and catabolism in recombinant *Saccharomyces cerevisiae*. *Biotechnol Biofuels* 5(1):14.
2. Demeke MM, et al. (2013) Development of a D-xylose fermenting and inhibitor tolerant industrial *Saccharomyces cerevisiae* strain with high performance in lignocellulose hydrolysates using metabolic and evolutionary engineering. *Biotechnol Biofuels* 6(1):89.
3. Carter Z, Delneri D (2010) New generation of loxP-mutated deletion cassettes for the genetic manipulation of yeast natural isolates. *Yeast* 27(9):765–775.
4. Güldener U, Heck S, Fielder T, Beinhauer J, Hegemann JH (1996) A new efficient gene disruption cassette for repeated use in budding yeast. *Nucleic Acids Res* 24(13):2519–2524.
5. Liang H, Gaber RF (1996) A novel signal transduction pathway in *Saccharomyces cerevisiae* defined by Snf3-regulated expression of *HXT6*. *Mol Biol Cell* 7(12):1953–1966.
6. Becker J, Boles E (2003) A modified *Saccharomyces cerevisiae* strain that consumes L-Arabinose and produces ethanol. *Appl Environ Microbiol* 69(7):4144–4150.

Table S4. Primers used in this work

Name	Sequence*	Description
del_GLK1_F	CCGCCCGACAGGGTAACATA	Forward primer for amplification of a *kanMX*-deletion cassette for *GLK1*
del_GLK1_R	AGTACGCCCCCTTGGAAGTG	Reverse primer for amplification of a *kanMX*-deletion cassette for *GLK1*
A1_GLK1	TAGACATGCTGCTTGCAAC	Forward primer for verification of a *GLK1* deletion (upstream)
A2_GLK1	TTCCTTTGGTGGAGCTAGAC	Reverse primer for verification of a *GLK1* deletion (ORF)
A4_GLK1	TTCGGACCTTAGCGGAGAG	Reverse primer for verification of a *GLK1* deletion (downstream)
del_HXK2_F	CTTTGATTGCGAGATCCACG	Forward primer for amplification of a *kanMX*-deletion cassette for *HXK2*
del_HXK2_R	CGTTCGTTCCAGAATTATCACG	Reverse primer for amplification of a *kanMX*-deletion cassette for *HXK2*
A1_HXK2	GCACCGGGCAATAAACCGG	Forward primer for verification of a *HXK2* deletion (upstream)
A2_HXK2	CAAAGTACCGGTAGTGTCGTTTATC	Reverse primer for verification of a *HXK2* deletion (ORF)
A4_HXK2	CGGGTATGAAGTGGTTGTGAGAATTAG	Reverse primer for verification of a *HXK2* deletion (downstream)
del_HXK1_F	**ATGGTTCATTTAGGTCCAAAGAAACCACAGGCTAGAAAGGGT TCCATGGC**TTCGTACGCTGCAGGTCGAC	Forward primer for amplification of a *hphNT1*-deletion cassette for *HXK1* from pZC1
del_HXK1_R	**TTAAGCGCCAATGATACCAAGAGACTTACCTTCGGCAATTCTTTTTT CGG**GCATAGGCCACTAGTGGATCTG	Reverse primer for amplification of a *hphNT1*-deletion cassette for *HXK1* from pZC1
A1_HXK1	CAAGGTCTCGCTGTCAACTG	Forward primer for verification of a *HXK1* deletion (upstream)
A2_HXK1	CTAGACCATGGGATGCAACT	Reverse primer for verification of a *HXK1* deletion (ORF)
A4_HXK1	CCTGGAAGTAGGTGCCCTTG	Reverse primer for verification of a *HXK1* deletion (downstream)
del_YLR446w_F	**ATGACAATTGAAAGCACTCTAGCTCGGGAATTA GAAAGCTTGATTTTACC**TTCGTACGCTGCAGGTCGAC	Forward primer for amplification of a *hphNT1*-deletion cassette for *YLR446w* from pZC1
del_ YLR446w _R	**TTATTGAACTTGGTTGTCTGATTTGTTCAAGTAGGTGG CTATTGCAGCGCC**GCATAGGCCACTAGTGGATCTG	Reverse primer for amplification of a *hphNT1*-deletion cassette for *YLR446w* from pZC1
A1_ YLR446w	CAAGCCTTCGTCAGCATTAC	Forward primer for verification of a *YLR446w* deletion (upstream)
A4_ YLR446w	GCACAAAACCAAAGAGAAAG	Reverse primer for verification of a *YLR446w* deletion (downstream)
K2_kanMX	TTGTCGCACCTGATTGCCCG	Reverse primer for detection of an genome-integrated *kanMX* deletion cassette
K3_kanMX	GATAATCCTGATATGAATAAATTGC	Forward primer for detection of an genome-integrated *kanMX* deletion cassette
K2_hphNT1	GAAAGCACGAGATTCTTC	Reverse primer for detection of an genome-integrated *hphNT1* deletion cassette
K3_hphNT1	TACACAAATCGCCCGCAGAAG	Forward primer for detection of an genome-integrated *hphNT1* deletion cassette
A1_PYK2	CATCCTCTACGTCCATTGTAAG	Forward primer to confirm pAF-HD8.3 integration into *PYK2* (upstream)
A2_PYK2	ACCCACATCCGATACTTCAG	Reverse primer for verification of *PYK2* replacement by pAF-HD8.3 (ORF)
A3_PYK2	AGTATCGGATGTGGGTAACG	Forward primer for verification of *PYK2* replacement by pAF-HD8.3 (ORF)
A4_PYK2	CCAGACTGTGCGTAAACTTG	revers primer to confirm pAF-HD8.3 integration into *PYK2* (downstream)
K2_pAF-HD8.3	ATACTAACGCCGCCATCC	revers primer to confirm pAF-HD8.3 integration into *PYK2* (cassette)
K3_pAF-HD8.3	CTAGGACCTTGTTGTGTG	Forward primer to confirm pAF-HD8.3 integration into *PYK2* (cassette)
Clon_kanR_F	**ATAACCCTGATAAATGCTTCAATAATATTGAAAAAGGAAGAGT**A TGAGCCATATTCAACGG	Forward primer for cloning of the kanamycin resistance gene
Clon_kanR_R	**AATCAATCTAAAGTATATATGAGTAAACTTGGTCTGACAG**T TAGAAAAACTCATCGAGCATC	Reverse primer for cloning of the kanamycin resistance gene

Table S4. Cont.

Name	Sequence*	Description
Clon_HXT7_F	**ATAAACACAAAAACAAAAAGTTTTTTTAATTTTAATCAAAAA** ATGTCACAAGACGCTGCTATTG	Forward primer for cloning of *HXT7*
Clon_HXT7_R	**GGAGGGCGTGAATGTAAGCGTGACATAACTAATTACA TGACTCGAG**TTATTTGGTGCTGAACATTCTC	Reverse primer for cloning of *HXT7*
Clon_GAL2_F	**AACACAAAAACAAAAAGTTTTTTTAATTTTAATCAAAAA**A TGGCAGTTGAGGAGAACAA	Forward primer for cloning of *GAL2*
Clon_GAL2_R	**GAATGTAAGCGTGACATAACTAATTACATGACTCGA G**TTATTCTAGCATGGCCTTGTACC	Reverse primer for cloning of *GAL2*
Amp_HXT7_F	ATGTCACAAGACGCTGC	Forward primer for amplification of the *HXT7* ORF
Amp_HXT7_R	TTATTTGGTGCTGAACATTC	Reverse primer for amplification of the *HXT7* ORF
Amp_GAL2_F	ATGGCAGTTGAGGAGAAC	Forward primer for amplification of the *GAL2* ORF
Amp_GAL2_R	TTATTCTAGCATGGCCTTG	Reverse primer for amplification of the *GAL2* ORF
HXT7_mut1-T213 _F	CTTGCTACCAATTGATGATTGBTGCCGGTATTTTCTTGG	Forward primer for mutagenesis of T213 to A/G/V in *HXT7*
HXT7_ mut1-T213_R	GTAACCCAAGAAAATACCGGCAVCAATCATCAATTGGTAG	Reverse primer for mutagenesis of T213 to A/G/V in *HXT7*
HXT7_mut2-T213 _F	CTTGCTACCAATTGATGATTTSTGCCGGTATTTTCTTGG	Forward primer for mutagenesis of T213 to S/C in *HXT7*
HXT7_ mut2-T213_R	GTAACCCAAGAAAATACCGGCASAAATCATCAATTGGTAG	Reverse primer for mutagenesis of T213 to S/C in *HXT7*
HXT7_mut3-T213 _F	CTTGCTACCAATTGATGATTRACGCCGGTATTTTCTTGG	Forward primer for mutagenesis of T213 to D/N in *HXT7*
HXT7_ mut3-T213_R	GTAACCCAAGAAAATACCGGCGTYAATCATCAATTGGTAG	Reverse primer for mutagenesis of T213 to D/N in *HXT7*
GAL2_mut1-T219 _F	CTTGTTATCAGCTGATGATTGBTGCAGGTATCTTTTTGG	Forward primer for mutagenesis of T219 to A/G/V in *GAL2*
GAL2_ mut1-T219_R	TAGCCCAAAAAGATACCTGCAVCAATCATCAGCTGATAAC	Reverse primer for mutagenesis of T219 to A/G/V in *GAL2*
GAL2_mut2-T219 _F	CTTGTTATCAGCTGATGATTTSTGCAGGTATCTTTTTGG	Forward primer for mutagenesis of T219 to S/C in *GAL2*
GAL2_ mut2-T219_R	TAGCCCAAAAAGATACCTGCASAAATCATCAGCTGATAAC	Reverse primer for mutagenesis of T219 to S/C in *GAL2*
GAL2_mut3-T219 _F	CTTGTTATCAGCTGATGATTRACGCAGGTATCTTTTTGG	Forward primer for mutagenesis of T219 to D/N in *GAL2*
GAL2_ mut3-T219_R	TAGCCCAAAAAGATACCTGCGTYAATCATCAGCTGATAAC	Reverse primer for mutagenesis of T219 to D/N in *GAL2*
HXT7_mut-N370 _F	CTATTGTCTTGGGTATTGTTNNNTTTGCTTCCACCTTTG	Forward primer for random mutagenesis of N370 in *HXT7*
HXT7_mut-N370_R	CCAACAAAGGTGGAAGCAAANNNAACAATACCCAAGAC	Reverse primer for random mutagenesis of N370 in *HXT7*
GAL2_mut-N376 _F	CCATTGTCATTGGTGTAGTCNNNTTTGCCTCCACTTTC	Forward primer for random mutagenesis of N376 in *GAL2*
GAL2_mut-N376_R	CTAAAGAAAGTGGAGGCAAANNNGACTACACCAATGAC	Reverse primer for random mutagenesis of N376 in *GAL2*
HXT7_N370F_F	CTATTGTCTTGGGTATTGTTTTCTTTGCTTCCACCTTTG	Forward primer for mutagenesis of N370 to F in *HXT7*
HXT7_N370F_R	CCAACAAAGGTGGAAGCAAAGAAAACAATACCCAAGAC	Reverse primer for mutagenesis of N370 to F in *HXT7*
GAL2_N376Y_F	CCATTGTCATTGGTGTAGTCTACTTTGCCTCCACTTTC	Forward primer for mutagenesis of N376 to Y in *GAL2*
GAL2_N376Y_R	CTAAAGAAAGTGGAGGCAAAGTAGACTACACCAATGAC	Reverse primer for mutagenesis of N376 to Y in *GAL2*
GAL2_I218G_F	TGTTATCAGCTGATGGGTACTGCAGGTATCTTTTTGG	Forward primer for mutagenesis of I218 to G in *GAL2*
GAL2_I218G_R	AAAGATACCTGCAGTACCCATCAGCTGATAACAAG	Reverse primer for mutagenesis of I218 to G in *GAL2*
GAL2_I218A_F	TGTTATCAGCTGATGGCTACTGCAGGTATCTTTTTGG	Forward primer for mutagenesis of I218 to A in *GAL2*
GAL2_I218A_R	AAAGATACCTGCAGTAGCCATCAGCTGATAACAAG	Reverse primer for mutagenesis of I218 to A in *GAL2*
GAL2_I218D_F	TGTTATCAGCTGATGGACACTGCAGGTATCTTTTTGG	Forward primer for mutagenesis of I218 to D in *GAL2*
GAL2_I218D_R	AAAGATACCTGCAGTGTCCATCAGCTGATAACAAG	Reverse primer for mutagenesis of I218 to D in *GAL2*
GAL2_I218K_F	TGTTATCAGCTGATGAAGACTGCAGGTATCTTTTTGG	Forward primer for mutagenesis of I218 to K in *GAL2*
GAL2_I218K_R	AAAGATACCTGCAGTCTTCATCAGCTGATAACAAG	Reverse primer for mutagenesis of I218 to K in *GAL2*
GAL2_I218F_F	TGTTATCAGCTGATGTTCACTGCAGGTATCTTTTTGG	Forward primer for mutagenesis of I218 to F in *GAL2*
GAL2_I218F_R	AAAGATACCTGCAGTGAACATCAGCTGATAACAAG	Reverse primer for mutagenesis of I218 to F in *GAL2*
GAL2_I222G_F	ATGATTACTGCAGGTGGTTTTTTGGGCTACTGTAC	Forward primer for mutagenesis of I222 to G in *GAL2*
GAL2_I222G_R	ACAGTAGCCCAAAAAACCACCTGCAGTAATCATCAGC	Reverse primer for mutagenesis of I222 to G in *GAL2*
GAL2_I222A_F	ATGATTACTGCAGGTGCTTTTTTGGGCTACTGTAC	Forward primer for mutagenesis of I222 to A in *GAL2*
GAL2_I222A_R	ACAGTAGCCCAAAAAAGCACCTGCAGTAATCATCAGC	Reverse primer for mutagenesis of I222 to A in *GAL2*
GAL2_I222D_F	ATGATTACTGCAGGTGACTTTTTGGGCTACTGTAC	Forward primer for mutagenesis of I222 to D in *GAL2*
GAL2_I222D_R	ACAGTAGCCCAAAAAGTCACCTGCAGTAATCATCAGC	Reverse primer for mutagenesis of I222 to D in *GAL2*
GAL2_I222K_F	ATGATTACTGCAGGTAAGTTTTTGGGCTACTGTAC	Forward primer for mutagenesis of I222 to K in *GAL2*
GAL2_I222K_R	ACAGTAGCCCAAAAACTTACCTGCAGTAATCATCAGC	Reverse primer for mutagenesis of I222 to K in *GAL2*
GAL2_I222F_F	ATGATTACTGCAGGTTTCTTTTTGGGCTACTGTAC	Forward primer for mutagenesis of I222 to F in *GAL2*
GAL2_I222F_R	ACAGTAGCCCAAAAAGAAACCTGCAGTAATCATCAGC	Reverse primer for mutagenesis of I222 to F in *GAL2*
GAL2_I222Q_F	ATGATTACTGCAGGTCAATTTTTGGGCTACTGTAC	Forward primer for mutagenesis of I222 to Q in *GAL2*
GAL2_I222Q_R	ACAGTAGCCCAAAAATTGACCTGCAGTAATCATCAGC	Reverse primer for mutagenesis of I222 to Q in *GAL2*
GAL2_Y446W_F	TTTTATATTTTCTGTTGGGCCACAACCTGGGCGCC	Forward primer for mutagenesis of Y446 to W in *GAL2*
GAL2_Y446W_R	CGCCCAGGTTGTGGCCCAACAGAAAATATAAAAACAGG	Reverse primer for mutagenesis of Y446 to W in *GAL2*
GAL2_F350A_F	GGTAACAATTATTTTGCTTACTACGGTACCGTTATTTTCAAGTC	Forward primer for mutagenesis of F350 to A in *GAL2*
GAL2_F350A_R	TAACGGTACCGTAGTAAGCAAAATAATTGTTACCGG	Reverse primer for mutagenesis of F350 to A in *GAL2*
GAL2_F350D_F	GGTAACAATTATTTTGACTACTACGGTACCGTTATTTTCAAGTC	Forward primer for mutagenesis of F350 to D in *GAL2*
GAL2_F350D_R	TAACGGTACCGTAGTAGTCAAAATAATTGTTACCGG	Reverse primer for mutagenesis of F350 to D in *GAL2*
GAL2_F350G_F	GGTAACAATTATTTTGGTTACTACGGTACCGTTATTTTCAAGTC	Forward primer for mutagenesis of F350 to G in *GAL2*
GAL2_F350G_R	TAACGGTACCGTAGTAACCAAAATAATTGTTACCGG	Reverse primer for mutagenesis of F350 to G in *GAL2*

Table S4. Cont.

Name	Sequence*	Description
GAL2_F350K_F	GGTAACAATTATTTTAAGTACTACGGTACCGTTATTTTCAAGTC	Forward primer for mutagenesis of F350 to K in *GAL2*
GAL2_F350K_R	TAACGGTACCGTAGTACTTAAAATAATTGTTACCGG	Reverse primer for mutagenesis of F350 to K in *GAL2*
GAL2_F350L_F	GGTAACAATTATTTTTTGTACTACGGTACCGTTATTTTCAAGTC	Forward primer for mutagenesis of F350 to L in *GAL2*
GAL2_F350L_R	TAACGGTACCGTAGTACAAAAAAATAATTGTTACCGG	Reverse primer for mutagenesis of F350 to L in *GAL2*
GAL2_F350M_F	GGTAACAATTATTTTATGTACTACGGTACCGTTATTTTCAAGTC	Forward primer for mutagenesis of F350 to M in *GAL2*
GAL2_F350M_R	TAACGGTACCGTAGTACATAAAATAATTGTTACCGG	Reverse primer for mutagenesis of F350 to M in *GAL2*
GAL2_F350W_F	GGTAACAATTATTTTTGGTACTACGGTACCGTTATTTTCAAGTC	Forward primer for mutagenesis of F350 to W in *GAL2*
GAL2_F350W_R	TAACGGTACCGTAGTACCAAAAATAATTGTTACCGG	Reverse primer for mutagenesis of F350 to W in *GAL2*
GAL2_F350Y_F	GGTAACAATTATTTTTACTACTACGGTACCGTTATTTTCAAGTC	Forward primer for mutagenesis of F350 to Y in *GAL2*
GAL2_F350Y_R	TAACGGTACCGTAGTAGTAAAAATAATTGTTACCGG	Reverse primer for mutagenesis of F350 to Y in *GAL2*

*Sequences that are homologous to target sequences (for recombinatorial cloning or genomic deletion/integration) are printed in bold; the mutated codon in primers for site-directed mutagenesis is underlined.